Eur. Phys. J. D (2014)
DOI: 10.1140/epjd/e2014-50319-8

THE EUROPEAN PHYSICAL JOURNAL D

Regular Article

Intense ion beam generation in a diode with explosive emission cathode in self-magnetically insulated mode

Alexander Pushkarev[a,b], Yulia Isakova, and Iliya Khailov

Tomsk Polytechnic University, 30, Lenin Ave, 634050 Tomsk, Russia

Received 22 April 2014 / Received in final form 18 June 2014
Published online (Inserted Later) – © EDP Sciences, Società Italiana di Fisica, Springer-Verlag 2014

Abstract. This paper presents a review of experimental studies on pulsed intense ion beam generation in self-magnetically insulated diodes with an explosive emission cathode. The experiments were carried out with the TEMP-4M accelerator operating in double-pulse mode: the first pulse is of negative polarity (300–500 ns, 100–150 kV), and this is followed by a second pulse of positive polarity (150 ns, 250–300 kV). The ion beam energy density is 0.5–5 J/cm^2 depending on the diode geometry. We have developed a new spiral geometry of the diode. In a spiral diode it is possible to increase the efficiency from 5–9% (previously studied diodes) up to 20–25%. We conducted a study on shot-to-shot variation in the ion beam parameters. It was found that the standard deviation of the energy density does not exceed 11%, whilst the same variation for ion current density was 20–30%. Focusing properties of an ion beam have been significantly improved by using a metal shield on the grounded electrode. Use of the shield on the grounded electrode provides decrease in the beam divergence from 11° to 7.5–8°.

1 Introduction

The development of advanced materials with preselected properties is one of the main goals of materials research. Of special interest are electronics, high-temperature and superhard materials for various applications, as well as alloys with improved wear, corrosion and mechanical resistance properties. The energetic charged particle, electron and ion beams offer the possibility of modifying the properties of the near-surface regions of materials without seriously affecting their bulk [1,2]. Among these pulsed beam techniques, high-intensity pulsed ion beams (PIB) [3–5] offer some essential advantages over electron or laser pulse treatment. Pulsed ion beams with the energy densities 1–10 J/cm^2 and the duration within 10 ns–1 μs provide intense heating and cooling of the near-surface layers of irradiated targets with a rate of more than 10^9 K/s. Typical thickness of such a layer is 0.1–10 μm [5]. This allows compounds and structures to be realized in surface layers which cannot be made by traditional industrial methods.

Intense ion beams are usually produced using diodes with external magnetic insulation or self-magnetic insulation [6,7]. There are two major problems to overcome for the effective production of intense ion beams: (1) suppression of the electronic component of diode current and (2) the formation of dense plasma ($n_i > 10^{14}$ cm^{-3}) on the anode surface.

After application of high voltage pulse to the diode and formation of cathode and anode plasma, generation of electron and ion current occurs simultaneously. The expressions for the electron and ion current densities in the planar diode can be defined based on the Child-Langmuir "3/2" law [8]:

$$J_e = \frac{4\varepsilon_0\sqrt{2e}}{9\sqrt{m}}\frac{U^{3/2}}{d^2(t)} = 2.33\times10^{-6}\frac{U^{3/2}}{[d_0 - vt]^2} \quad (1)$$

$$J_{ion} = \frac{4\varepsilon_0\sqrt{2z}}{9\sqrt{M}}\frac{U^{3/2}}{[d_0 - vt]^2} \quad (2)$$

where ε_0 is the permittivity of free space, e and m, z and M are the charge and mass of the electron and ion, respectively, U is the voltage across the diode, and d is the diode gap spacing, d_0 is the actual distance between the cathode and the anode, and v is the expansion velocity of plasma equations (1) and (2) are correct for non-relativistic voltages and cathode dimensions much larger than d_0.

According to the equations, the largest current density of protons is 2.3% of the electron current density. The density of heavier ions is lower. This means that around 98% of the energy supplied to the diode is wasted in accelerating electrons, rather than ions.

In 1973 Sudan and Lovelace [9] first suggested constructing a pulsed ion diode with applied magnetic insulation. The magnetic field causes the electron trajectory to bend (under the Lorentz force) by 90° ($B > B_{cr}$) as the electrons drift across the electric field in the A-C gap. If the electron transit time in the A-C gap exceeds that

[a] e-mail: aipush@mail.ru
[b] e-mail: isakova_yulia@tpu.ru

of ions, then the energy consumption to electrons can be reduced significantly. With the closed electron drift trajectory the efficiency of ion beam generation can reach up to 90%. This idea was confirmed experimentally in 1976 by Dreike et al. [10]. However, an additional energy source for the formation of the magnetic field increases the power consumption of the generator. For instance, for a total ion beam energy of 80–90 J per pulse, up to 500 J is required from the magnetic field source [11]. The efficiency of the ion beam generation, taking into account the energy consumed to form the magnetic field, does not exceed 10–15%. In some geometries, the magnetic field provided by current flowing through the cathode, is sufficient to provide self magnetic insulation, eliminating the need for an external source. In 1977, Humphries [12] first suggested the construction of an ion diode with self-magnetic insulation. A transverse magnetic field is formed in the A-C gap by the self-diode current when the current flows through the cathode. This significantly simplifies the construction of the pulsed ion beam generator, but the efficiency of ion current generation in diodes with self-magnetic insulation does not exceed 5–10%, which limits their application.

As for the second problem of plasma formation on the anode surface, the surface plasma is generated by a process known as explosive electron emission [13]. In 1980, Logachev et al. [14] suggested using this phenomenon for formation of dense plasma on the anode surface. They developed a bipolar pulse high voltage generator with nanosecond pulse duration [15]. The first pulse is used for the formation of the explosive-emission plasma on the surface of the potential electrode (cathode). The second pulse is used for the extraction of ions from the plasma. It was recently shown by several authors [16] that the uniformity of the plasma formation of the cathode surface and, respectively, the uniformity of the extracted electron and ion beam depends strongly on the on the accelerating electric field growth rate dE/dt.

Our studies showed that duration of the formation of a uniform plasma layer on the 100–200 cm^2 cathode surface area is 300–400 ns [17]. Explosive electron emission as a method for plasma formation provides a long (up to 10^6 pulses) operational life of the diode. At the time when diode voltage reverses polarity, the removal of plasma from the A-C gap takes place (plasma erosion effect) [17]. The duration of plasma erosion does not exceed 8–10 ns. As a result of plasma erosion effect the A-C spacing is restored to its original geometrical value and then replenished again due to plasma expansion [18].

In spite of much progress in the development of intense ion beam sources, many processes in an ion diode with self-magnetic insulation have not been researched enough. This can be explained in the following way: during the 1980–2000 years, the main application of pulsed ion beams was in controlled thermonuclear fusion investigations. The production of ion beams with maximum current density and a pulse power of more than 10^{12} W was mostly attempted. This paper gives a review of recent achievements in understanding the mechanisms involved in intense ion beam generation in self magnetically insulated diodes. We present the analysis of data obtained using an intense ion beam accelerator at Tomsk Polytechnic University, and also of a number of pulsed ion diodes known in the literature.

2 Experimental apparatus and diagnostics

The experiments have been conducted using the TEMP-4M [19] pulsed ion accelerator configured in bipolar pulse operation mode. The generator configured in double-pulse mode forms two pulses of opposite polarity: the first pulse is of negative polarity (300–600 ns, 100–150 kV), and this is followed by a second pulse of positive polarity (150 ns, 250–300 kV). The accelerator consists of the Marx generator, double transmission line (Blumlein) and vacuum ion diode with self-magnetic insulation of electrons. The ion beam energy density is 0.5–5 J/cm^2 (for different diode geometries), pulse repetition rate is 5–10 pulses/min. In a recent modification to the accelerator [20], we removed the charging inductor from the Blumlein generator. It allowed us to increase the energy delivered to the load from that stored in the Blumlein by a factor of 1.5 and optimize plasma formation on the cathode surface. To improve the statistical performance of the main spark gap in the Blumlein generator we changed the regime of its operation from a self-triggered mode to an externally triggered mode. In the new arrangement the first voltage pulse at the output of Blumlein was used to trigger the main spark gap. The new trigatron-type regime of the main spark gap operation showed a good stability of breakdown voltage and thus allowed to stabilize the duration of the first pulse. The standard deviation of the breakdown voltage and duration of first pulse was decreased from 10% to 2% in a set of 50 pulses [21].To improve the reproducibility of the first pulse duration (when the main spark gap was operated in self-breakdown mode) the hold on voltage of the main gap was set to a level of 0.7–0.8 from the maximum voltage at the output of the Marx generator. Concurrently, change in breakdown voltage in 4%–5% resulted in change in the first pulse duration in 6%–7%. The energy stored in the Marx generator was 4–5 kJ, while the energy stored in Blumlein was 1.2 kJ. Utilization of the externally triggered mode of the main spark gap also allowed for a decrease in the charging voltage of the Blumlein to a 0.9–0.95 of self-breakdown voltage of the main spark gap while the energy stored in the Marx generator was decreased from 4 kJ to 2.5 kJ. At the same time the energy stored in Blumlein remained the same. It allowed us to improve the shot to short stability of the accelerator and increase the service life of the accelerator components. The schematic of the strip planar diode chamber with various diagnostics and waveforms of accelerating voltage, total diode current and ion current density measured at 17 cm downstream from the diode are shown in Figure 1.

Information on the diode connection, diagnostic equipment used in the TEMP-4M accelerator and calibration can be found in our previous papers [22,23]. The voltage applied to the diode was measured by a high-frequency high-voltage divider which was installed in front of the

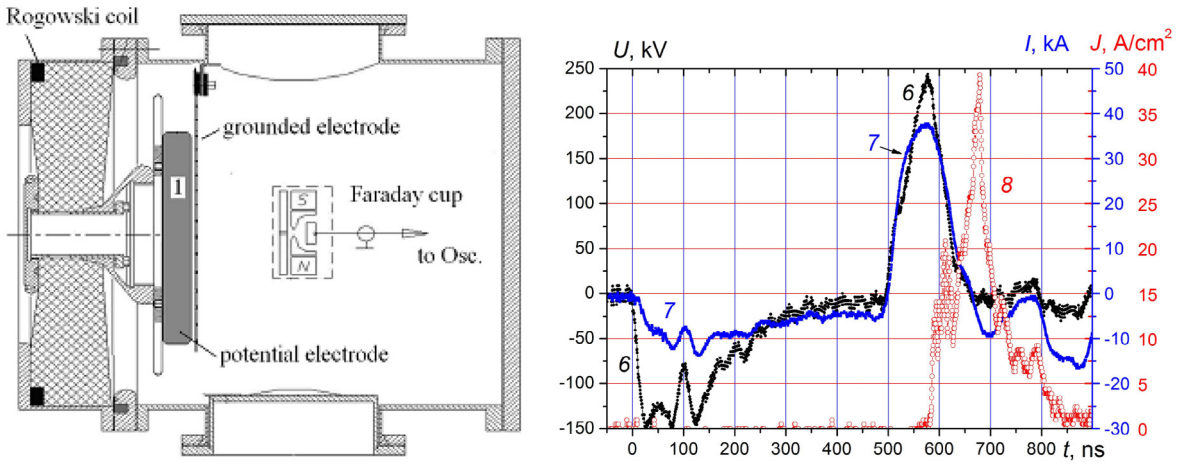

Fig. 1. Schematic of the strip planar diode and waveforms of accelerating voltage (6), total diode current (7) and ion current density (8) of a strip planar diode with self-insulation; A-C gap spacing of 8 mm.

diode connection. The total current in the diode was measured using a Rogowski coil (Fig. 1). The ion current density was measured by a magnetically insulated Faraday cup ($B = 0.4$ T) placed 4–17 cm (depending on diode geometry) downstream from the grounded electrode (Fig. 1). The electrical signals coming from the sensors were recorded with a Tektronix 2024B oscilloscope (250 MHz, 5 GSPS). The energy density distribution was measured using the infrared imaging diagnostic of thin metal targets intercepting the beam [24]. As the target, a 100 μm stainless steel foil was used placed 90 mm downstream from the cathode. All studied diode geometries with a graphite explosive emission cathodes worked effectively with the pressure in a diode chamber of 0.1 Pa and had an operational lifetime of up to 10^6 shots, since there is negligible degradation of the graphite electrode surface, which make it promising for various technological applications.

3 Electron current suppression in a self-magnetically insulated diode

To achieve high efficiency of ion beam production in a diode one needs to suppress the electron component of total diode current. In order to effectively suppress the electron current the electron transit time in the A-C gap must exceed that of ions. In a self-magnetically insulated diode transverse magnetic field is formed in the A-C gap by the self-diode current flowing through the cathode which is grounded at one end only. The electrons drift in crossed $E \times B$ field towards the free (not grounded) end of the cathode, provided that magnetic induction is sufficient to confine electrons along the cathode. A simplified mechanism illustrating electron drift is shown in Figure 2.

In a diode with an externally applied magnetic field it is easy to realize closed electron drift in the gap, allowing electrons to drift perpendicular to the electric field lines during the whole voltage pulse. As a result, the efficiency of ion current generation in such diodes is more than 80%. In a self-magnetically insulated diode the realization of closed electron drift is difficult since one end of the cathode must be connected to the diode chamber. For self-magnetically insulated diodes effective suppression of the electron current is possible by reducing the electron drift velocity and (or) increasing the length of the diode. The average electron transit time can be calculated (taking into account the reduction of the A-C gap [25]) and the effect of plasma erosion [17] when accelerating voltage reverses polarity), as:

$$\tau_e = \frac{L}{2v_{dr}(t)} = \frac{LB(t)}{2E(t)} = \frac{L\left[d_0 - v(t-t_0)\right]B(t)}{2U(t)} \qquad (3)$$

where L is the length of the electrode, v_{dr} is the electron drift velocity, E is the electric field strength, B is the magnetic induction, t is the first pulsed duration ($t_0 =$ 500 ns in Fig. 1).

In order to calculate electron transit time in A-C gap one needs to know the distribution of self-magnetic field inside the AC gap (see Eq. (3)). In an ion diode with self-magnetic insulation, it is difficult to measure the induction, since magnetic field is formed in the diode by current flowing though the electrode when a voltage of more than 200 kV is applied. The simulation of magnetic induction in the A-C gap was made using the Quick field software [26]. Figure 3 shows the distribution of the magnetic field in the cross section of the A-C gap.

The simulation is performed for a 40 mm × 1 mm conducting plate made of stainless steel with a current of 10 kA. The surface of the grounded electrode corresponds to $x = 0$ on curve 2 in Figure 3b. The calculation is performed taking into account strengthening of magnetic field due to conductive material of potential electrode (graphite).

The time dependent magnetic induction in the A-C for a planar diode was determined as: $B(t) = 0.014I(t)$, T, with current in kA.

Assuming that ions are uniformly accelerated in the A-C gap, the maximum velocity that ions reach moving

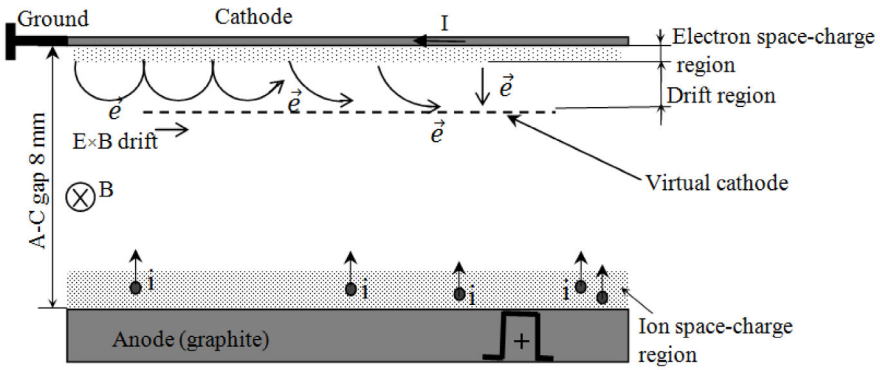

Fig. 2. Illustration of magnetized electron drift in a self-magnetically insulated ion diode.

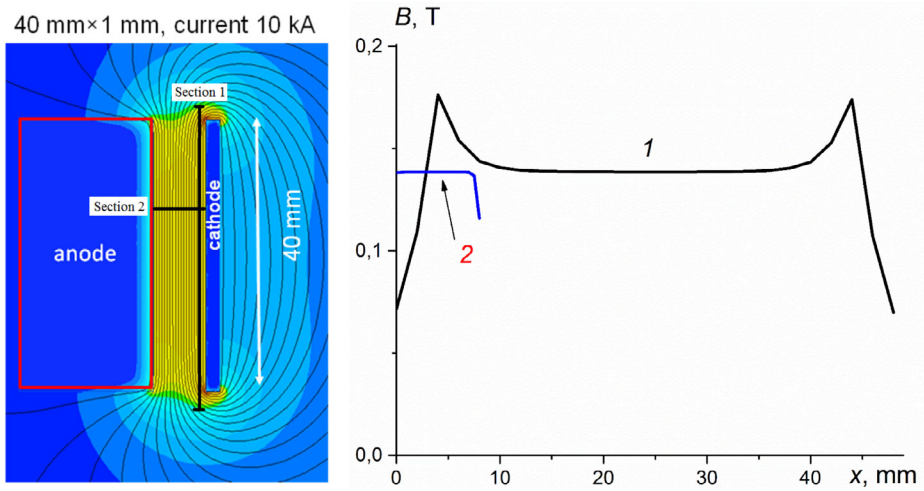

(a) (b)

Fig. 3. Simulation of magnetic field pattern in cross section of the diode (a). Distribution of magnetic induction along the A-C gap (section 1–curve 1 and section 2-curve 2) (b).

across the A-C gap is $\nu_{\max} = a\tau_{ion}$. Hence, the transit time of ions in the gap τ_{ion} (taking into account the reduction of the A-C gap and the effect of plasma erosion) is given by:

$$\tau_{ion}(t) = \frac{v_{\max}}{a} = \sqrt{\frac{2zU}{M}}\frac{d(t)M}{Uz} = \frac{[d_0 - v(t-t_0)]\sqrt{2M}}{\sqrt{zU}}$$

where a is the acceleration in the electric field.

Figure 4 shows the calculation of electron and ion transit times in the A-C gap for the strip planar diode.

The calculation was performed for singly ionized carbon ions and protons, with the average length of the electron drift being 11 cm (half of the diode length) and A-C gap spacing of 8 mm. The simulation of magnetic induction in the A-C gap was made using the QuickField software [26]. Studies show that electrons transit time in the A-C gap for strip diodes is close to that of protons and even lower for carbon ions. The results suggest a low efficiency of magnetic insulation. The electron drift along the A-C gap does not provide suppression of the electron current. The increase in voltage on the anode leads to an increase in the electron current in the diode (see Eq. (1)), which consequently increases the magnetic induction because of the increase in current through the cathode. However, it does not significantly affect the electron drift velocity (see Eq. (3)). Table 1 summarizes the

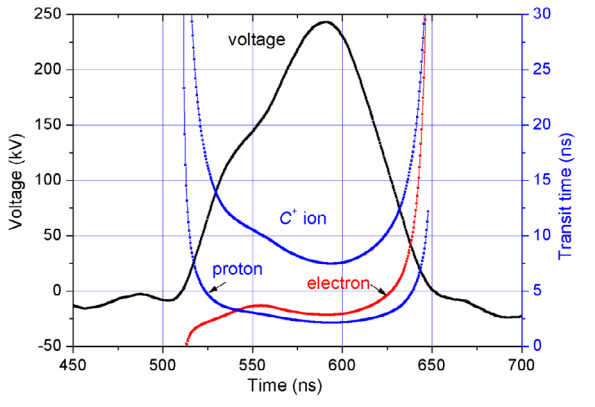

Fig. 4. Waveforms of the accelerating voltage, transit time of C^+ ions, protons and electrons in the A-C gap.

Table 1. Characteristics of different self-magnetically insulated diodes.

Name of the accelerator	Type of ions	B_{cr}, T	B_{min}, T	$B_{A\text{-}K}$, T	I_i/I_e	CL	$K1$	$K2$	Reference
Mite	protons	0.27–1.6	4	4–7.5	10%	2.3%	–	4.3	Vandevender et al. 1981 [27]
POLLUX		–	–	1.5 B_{Kp}	18–28%	2.3%	1.4	4–6	K.W. Zieher [28]
PARUS		0.25–0.38	1.8	0.31–0.73	15–20%	2.3%	2–2.5	3–4	Bystritskii et al., 1991 [29]
TONUS, VERA		0.19	0.23	0.18	27–33%	4.6%	1.9–2.3	2–5	Bystritskii et al., 1985 [30]
ETIGO-1		0.25	1.75	0.73	29%	2.3%	1.26	10	Yoshikawa et al., 1984 [31]
TEPP-4M. Strip planar diode	C^+ (85%) and protons	0.17–0.22	1.8–2.2	0.7	5–6%	0.7%	1.5–2	5–8	Pushkarev et al., 2010 [23]
TEPP-4M. Strip focusing diode		0.17–0.22	1.8-2.2	0.7	8–9%	0.7%	1.5–2	5–8	Pushkarev et al., 2012 [38]
TEPP-4M. Annular diode		0.16–0.21	0.76–0.93	0.4–0.6	15–20%	0.7%	4–5	–	Pushkarev et al., 2012 [32]
TEPP-4M. Spiral diode		0.26	0.34	0.8	17–20%	0.7%	2–2.5	–	Pushkarev et al., 2012 [33]
TEPP-4M. Spiral diode with closed electron drift		0.24	0.34	3.1	30–40%	0.7%	2.3–2.6	–	Pushkarev et al., 2013 [34]

B_{cr} – Critical magnetic induction.
B_{min} – Magnetic induction at which electron transit time in the A-C gap equals that of ions.
B_{AK} – Magnetic induction in the A-C gap near the cathode (electron drift region).
CL – Ratio of calculated ion current density (Eq. (2)) to calculated electron current density (Eq. (1)).
K_1 – Ratio of calculated electron current density (Eq. (1)) to experimental electron current density.
K_2 – Ratio of experimental ion current density to calculation by equation (2).

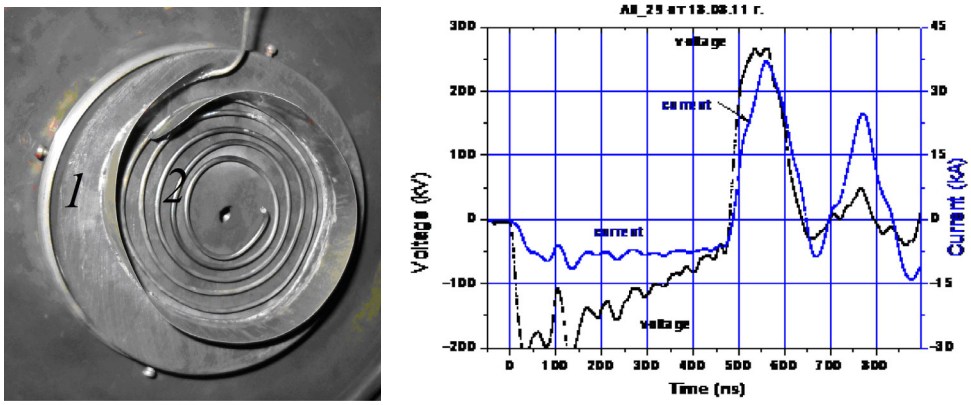

Fig. 5. Photograph of spiral diode: anode (1), cathode (2). Waveforms of the accelerating voltage, total current in the spiral diode.

characteristics of PIB generation and efficiencies of different self-magnetically insulated diodes.

Analysis of different diodes with self-magnetic insulation shows that in most diodes quoted in the literature transit times of ions exceeds that of electrons, thus suppression of electron current is not provided by self-magnetic field ($B_{AK} < B_{min}$, see Tab. 1). However, measured total current in the diode during the pulse is less than calculated C-L current for electrons ($K1 \geqslant 2$ in Tab. 1). The results suggest that a decrease in electron current observed in the experiments is not due to that electron transit time in the gap increases that of ions, but due to some other effect.

4 A spiral ion diode with self magnetic insulation

As mentioned above, for self-magnetically insulated diodes effective suppression of the electron current is possible by increasing the length of the diode and (or) reducing the electron drift velocity. The length of the cathode can be easily increased by using a spiral geometry [33]. In a strip ion diode with self-magnetic insulation described elsewhere [19,23,24] the cathode is designed as a strip measuring 22 cm × 4.5 cm with the slits of 4 mm wide and 2 cm long, resulting in a transparency of 70%. The transverse magnetic field in the A-C gap is formed by self-diode current flowing through the cathode. The total current is distributed over the entire width of the cathode (4.5 cm), which reduces the current density over the cross section and consequently the magnetic induction in the A-C gap. A spiral geometry cathode allows one to increase the current density in the cross section of the winding, and thus also magnetic field close to its surface, providing a higher level of magneitc insulation. This increases the electron drift time along the length of the spiral (see Eq. (3)). A photograph of the spiral diode and typical waveforms of accelerating voltage and total diode current are shown in Figure 5.

The dimensions of the spiral cathode are an outer width of 14 cm, inner width of 5 cm, with a pitch of 0.8–1 cm and a total length for the wire of 150–170 cm. The anode is a flat disc of graphite 20 cm in diameter and 4 cm thick. The value of A-C gap spacing along the entire length of the diode was constant and equal to 7–8 mm. Figure 6 shows an infrared image on the target with the imprinted beam generated by a spiral diode and the material erosion pattern on the metal target, observed after 5 shots. As the target, a 100 μm stainless steel foil was used placed 90 mm downstream from the cathode.

One of the most important parameters of an ion diode from an industrial perspective is the efficiency, which in terms of energy is the ratio of the energy of the extracted ion beam, to the total energy supplied to the diode. Figure 7 shows the efficiencies determined for the spiral and planar self-magnetically insulated diodes.

The total ion beam energy (Y-axis) was calculated by integrating the energy density distribution across the target, which was obtained using an infrared imaging diagnostic. The energy supplied to the diode from the Blumline (X-axis) was calculated using the measured current and voltage waveforms. The increase in the electron drift time in the spiral diode led to an increase in the efficiency of ion beam generation up to 20%.

The high efficiency is achieved with a large value of magnetic induction in the gap ($B/B_{cr} \geqslant 5$). The magnetic field is formed by the self-diode current flowing though the spiral electrode. The simulation of magnetic induction in the A-C gap was made using the QuickField software [26]. Figure 8 shows a cross section of the magnetic induction in the gap for the spiral diode. The diameter of the wire in the spiral is 3 mm, the pitch of spiral is 10 mm, the total current thought the spiral is 40 kA.

Configuration of magnetic field lines surrounding adjacent turns in the spiral diode is similar to that obtained using a B_r applied magnetic field diode developed in reference [11].

Figure 9 shows the distribution of the magnetic induction along the gap on the distance of 1 mm from the grounded electrode (section A in Fig.) and critical magnetic induction (B_{cr}).

The induction of magnetic field in the A-C gap exceeds the critical induction by a factor of 3–3.5 on the

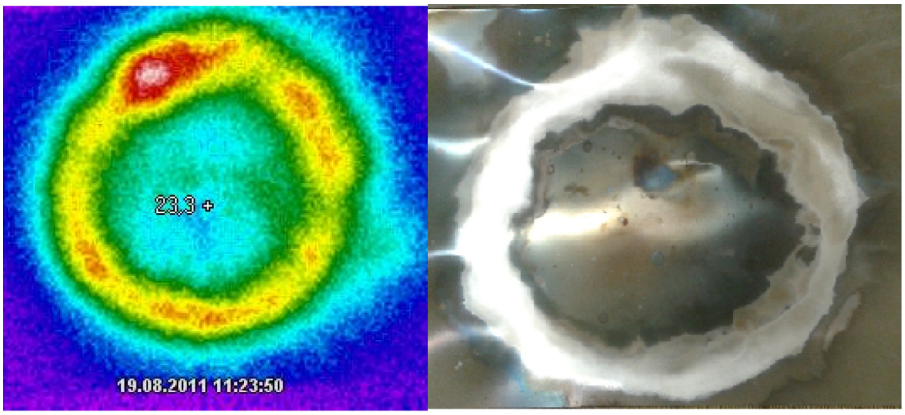

Fig. 6. Thermal imprint of the beam and the material erosion pattern on the metal target, observed after 5 shots.

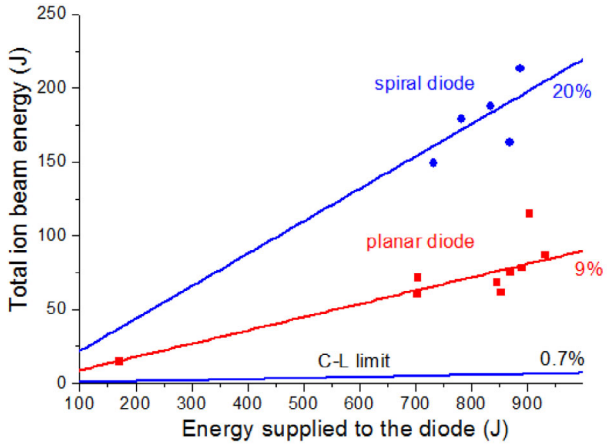

Fig. 7. Efficiency of ion beam production for diodes with self-magnetic insulation.

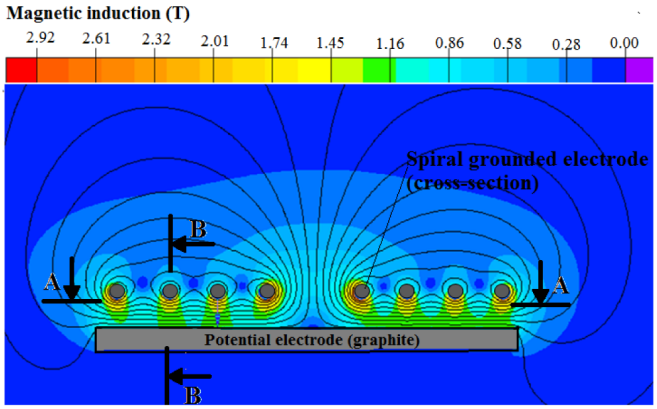

Fig. 8. Cross section of the magnetic induction in the A-C gap of the spiral diode.

first pulse and by a factor of 5–6 on the second pulse. The spiral geometry of the grounded electrode provides a higher transparency for ions, increasing the portion of the ion beam extracted from the A-C gap in to the transportation region by 80–90%.

As opposed to the strip focusing and planar diodes in the spiral diode magnetic induction in the A-C gap is much higher than the critical magnetic induction not only during the second pulse (when ions are accelerated), but also on the first pulse (see in Fig. 9). This allows one to estimate the duration of the drift of magnetized electrons during the first pulse. We used three charge collectors to measure the electron current at different positions along the surface of the diode. The photograph of the diode chamber with the charge collectors installed is shown in Figure 10. The diameter of the collector was 8 mm and the diameter of the hole in the lid was 4 mm. There was no biased voltage or insulating magnetic field applied to the collector. The electron current was recorded simultaneously by three collectors, located at a distance of 10 cm downstream from the diode (Fig. 10). One of the collectors was positioned at the center of the diode and the other two were located at a distance of 7 cm from the central collector, as shown in Figure 10.

In the absence of the magnetic field, we would expect similar readings between the three collectors. However the measurements showed that electron current was much higher towards the centre of the diode, being negligible at the edges. It is also delayed until much later in the pulse.

This supports the idea that electrons are confined by the magnetic field to drift along the length of the spiral towards the free end in the centre. The experimental results show that the duration of the drift of magnetized electrons on the first pulse exceeds 200–300 ns. It can be explained by the increase in the length of the electron drift and, consequently, increase in the in the electron transit time in the spiral diode.

5 Statistical analysis of the diode performance during ion beam generation

An important parameters of any intense ion beam accelerator, from an industrial perspective, is good reproducibility of the beam and a long lifetime under repetitive operation. With the ion current density of 40–100 A/cm^2,

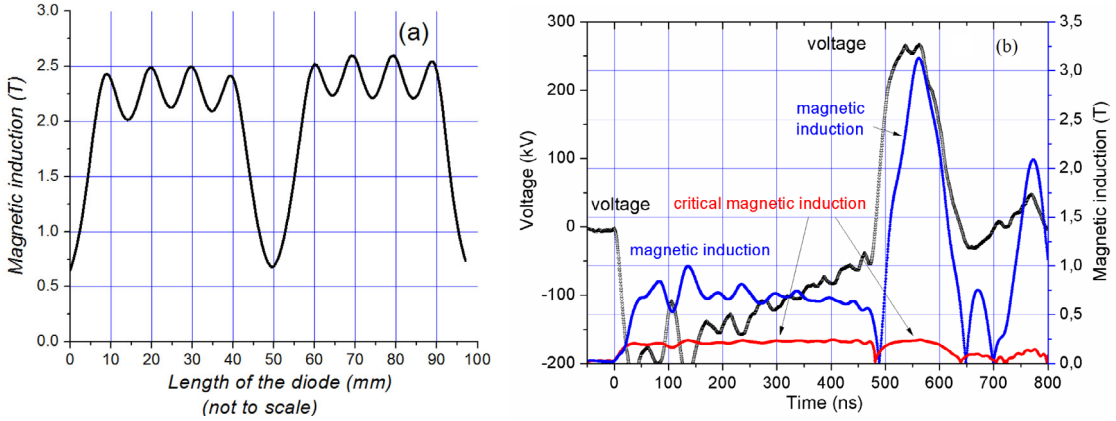

Fig. 9. Distribution of the magnetic induction along the A-C gap on 1 mm from the grounded electrode (a). Waveforms of accelerating voltage, magnetic induction in the A-C gap and the critical magnetic induction (b).

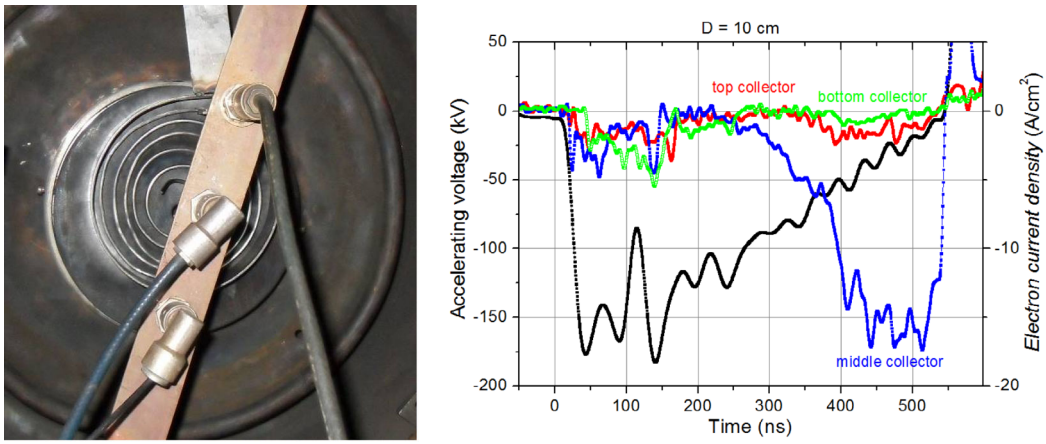

Fig. 10. The schematic of the measurement of the electron current by three charge collectors and waveforms of the accelerating voltage and electron current density on the first pulse, measured by three charge collectors.

accelerating voltage of 250–300 kV and pulse duration of 100–150 ns, the concentration of ions in PIB does not exceed 10^{12} cm^{-3}, therefore a significant factor affecting the properties of a treated specimen is the thermal effect of the beam, rather than ion implantation. Therefore, considerable attention should be paid to achieving good reproducibility of PIB energy density.

Data on the stability of ion diode with external magnetic insulation utilizing a polymer anode for experiments performed using the TEMP-6 accelerator (300–350 kV, 80 ns, 150–300 A/cm^2) were reported in references [35,36]. It was shown that parameter variation increases with the number of shots, being especially significant after more than 400 shots. The ion current density variation was about ±5% for $N \leqslant 200$, increasing to $\pm(15 \div 20)\%$ for $N \geqslant 400$. Ito et al. [37] observed a shot-to-shot variation in ion current density of about 20%. The poor reproducibility of the accelerated ion beam current density was attributed to the shot-to-shot variation of the plasma source.

In a previous paper [38] we presented the analysis of shot to shot reproducibility of the ion current density for the beam formed by a self-magnetically insulated ion diode with an explosive emission graphite cathode. It was found that the shot to shot variation in the ion current density was about 25–30%, whilst the diode voltage and current were comparatively stable with variation less than 10%. The statistical results of the reproducibility of the electrical parameters of the accelerator are summarized in Table 2.

It was shown that focusing of the ion beam reduces variations in ion current density to 18–20% [38]. However, the reproducibility of energy density for the same diode is much better. The results of a statistical analysis are shown in Figure 11 and summarized in Table 3. We measured energy density of the beam using the infrared imaging diagnostic. The time interval between measurements was 120 s to allow target temperature to equalize between shots.

A possible reason for a relatively good reproducibility of the energy density compared to ion current density for the same diode is the target ablation which can affect the results of the measurements. When the beam energy density exceeds the ablation threshold of the target, the energy absorbed by the target is less than the incident beam energy, because some energy is carried away in the ablated material [39]. This leads to an underestimation of the

Table 2. Statistical analysis of the electrical parameters for the TEMP-4M accelerator.

	Set 1	Set 2	Set 3	Set 4	Set 5	Standard deviation for 5 sets
Accelerating voltage, kV	242 ± 7%	241 ± 5.4%	258 ± 5.7%	255 ± 5%	258 ± 5.8%	5.8%
First pulse duration, ns	457 ± 9%	470 ± 9%	453 ± 11%	451 ± 10%	440 ± 13%	10%
Ion current density, A/cm^2	34 ± 20%	38 ± 27%	30 ± 27%	35 ± 29%	29 ± 29%	27%

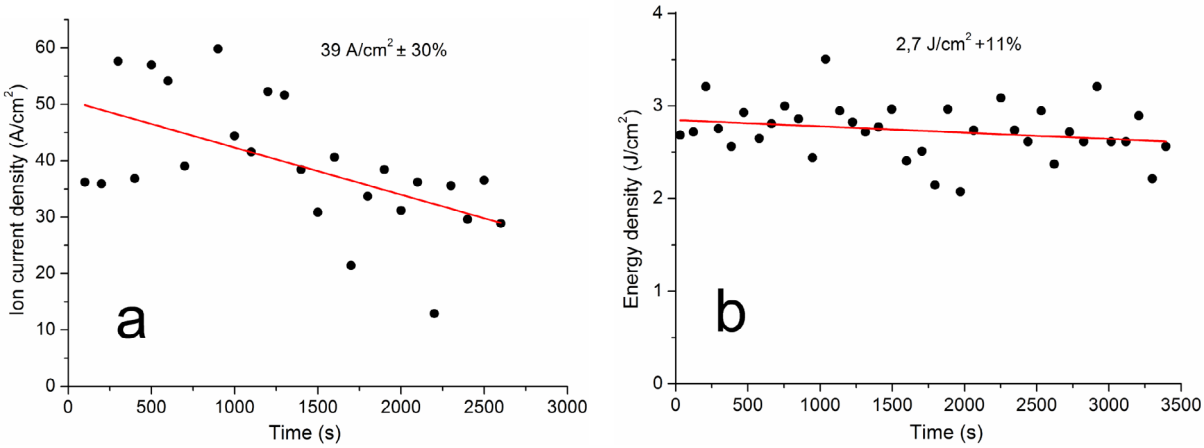

Fig. 11. The shot-to shot variation in the ion current density (a) and energy density (b).

Table 3. Statistical analysis of the electrical parameters for the TEMP-4M accelerator.

	Mean value and standard deviation			
	U, kV	I, kA	W, J	w, J/cm^2
Set 1	244 ± 9%	68 ± 8%	103 ± 11%	4.2 ± 8%
Set 2	–	66 ± 5%	100 ± 8%	3.8 ± 10%
Set 3	–	56 ± 4%	83 ± 10%	3.8 ± 9%
Set 4	255 ± 5%	59 ± 5%	66 ± 9%	2.7 ± 11%

beam energy density when measured by infrared imaging diagnostic, which also affects the results of statistics. We expect that variations in the amount of ablated material from shot to shot, would increase the standard deviation of energy density measured; therefore by reducing energy density so that it does not exceed the ablation threshold of the target we would expect to see reductions in the standard deviation. However, the measurements (see Tab. 3, sets 3 and 4) show that reduction in the beam energy density did not reduce standard deviation.

For statistical measurements of the energy density at the repetition rate of 5–6 pulses/s we developed acoustic diagnostics based on a piezoelectric transducer [40]. The results of measurements showed that the standard deviation of the energy density at a high repetition rate (time interval between measurements of 10 s) does not exceed 11%, which is close to that obtained with infrared imaging diagnostics (time interval between measurements is 120 s).

A previous study [38] showed that the correlations between the ion current density and the output parameters of the Blumlein are weak, with the determination coefficient (adj. R-Square in the program Origin 8) not exceeding 0.3–0.35, indicating that the shot-to-shot variations observed do not seem to be due to the reproducibility of the pulsed power system. However, the statistical analysis revealed the high correlation of the total beam energy and energy density with the total charge. Energy density and total energy of the beam are integral parameters, reflecting beam formation over the whole time of generation, therefore one should compare these to integral parameters for the Blumlein, such as the charge (time integral of current) transferred during the second pulse. Figure 12 shows the experimental data for strip planar and focusing diodes and a spiral diode at different A-C gap spacings. The total ion beam energy was measured using both a calorimeter and an infrared imaging diagnostic. The correlation observed was excellent for all gap spacing, with the coefficient of determination for the complete data set being 0.9.

The study showed that for all diodes except for the spiral diode, the relationship between the total beam energy and total charge carried by the beam can be described by the linear dependences and fits one line with a standard deviation of 7% at different A-C gap spacings. The dependence of the total beam energy on total charge is somewhat different for the spiral diode. These results suggest a fundamental difference between the two forms of

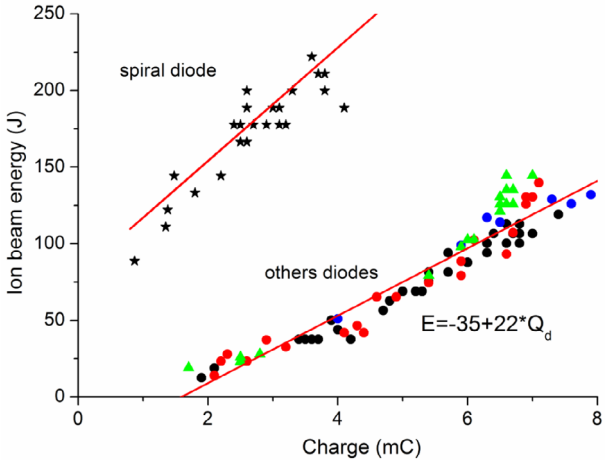

Fig. 12. Dependence of total PIB energy on the total charge for the strip focusing and planar diodes, a conical focusing diode, a spiral diode.

diode, the differences between which we explain by the increase in the length of the electron drift (the length of the grounded electrode in the spiral diode is 150–170 cm compared to 20–25 cm for the strip planar and focusing diodes) in the spiral diode.

6 Ion beam transportation and focusing

Modification of materials with high-thermal conductivity requires using PIB with an energy density higher than 4–5 J/cm^2 and pulse duration of 100–150 ns.

It is possible to obtain a high energy density on the target by focusing of the ion beam and eliminating beam scattering during transport In ion diodes geometric (ballistic) focusing is commonly used. Geometric focusing is achieved by curvature shape of the anode and cathode. However, while ions are propagated to the focus their deviation from the initial path occurs due to Coulomb repulsion, influence of electromagnetic fields, diffusive scattering, etc. [6].

A detailed study on intense ion beam focusing and propagation in different diodes is given in reference [41]. It is shown that magnetically insulated diodes exhibit a smaller ion beam divergence (ratio of the beam radius at half-height to the distance from the diode), amounting to 1–4°, in contrast to reflex diodes and pinch-diodes. An analysis of focussing issues of PIB generated in a magnetically insulated diode with hemispherical electrodes is given in reference [42]. The research conducted with the ETIGO-1 accelerator (1.2 MV, 240 kA, 50 ns) showed that PIB focusing properties are mainly affected by heterogeneous surface of the anode plasma and distortion of the electric field near the cathode. The defocusing of the beam is mainly due to the deviation angle. The deviation angle and hence the total divergence angle have been significantly reduced from 6° to 2.5° by improvement of the cathode structure.

The divergence angle amounted to 8° of an ion beam extracted from an applied B_r magnetically insulated diode (400 kV; 0.5 μs) was found in reference [39]. A study on ion beam focusing in a self-magnetically insulated diode was conducted with the PARUS accelerator (0.8 MB, 60 ns) by Bystritskii et al. in reference [29]. The authors point out that the beam divergence occurs due to presence of the magnetic field in the region of ion beam extraction through the slits in the cathode, that causes distortion of a virtual cathode surface. The half divergence angle, measured by a pin-hole camera was found to be ≈3°. In a self-magnetically insulated ion diode, developed by Zieher in reference [28] ion beam divergence was about 1.5°–3.6° for different anodes [43]. A necessary condition for current neutralization for an ion beam generated in a self-magnetically B_θ-insulated ion diode is derived in reference [44]. The requirement for which is the following: the magnetic field of the cathode outside the diode gap is small enough to still allow electrons to flow from the cathode along with the beam.

In spite of numerous studies on ion beam transport and focusing and a detailed analysis of the reasons for ion beam scattering, there are no experimental data about the influence of electromagnetic field in the transport region on ion beam focusing properties in self-magnetically insulated diodes. Self-magnetic field penetrates into a skin-layer depth in plasma of a space charge compensated ion flow, which causes the removal of low-energy neutralizing electrons from the beam and beam scattering. If the concentration of ions (and neutralizing electrons) is low, a skin-layer depth may compose an essential part of a beam diameter. Furman [11] suggested the use a metal shield for improving focusing properties of PIB, formed by an applied B_r magnetically insulated diode.

For effective ion beam transportation one needs to apply neutralization to create and to transport high-flux ion beams. A high concentration of PIB (10^{10}–10^{13} ion/cm^3) leads to a change in potential that may reach hundreds of kilovolts. A corresponding field (10^5–10^6 V/cm) causes the scattering of such a beam along its length [6]. For elimination of ion beam scattering one needs to reduce the beam-generated electric field by mixing low-energy electrons with the ions. The mobile electrons should be supplied to the beam volume at the outlet of the A-C gap. There are two ways to neutralize an ion beam with electrons. First, we can direct the beam through a dense plasma. The plasma electrons shift in position to compensate for the added positive charge. An alternative approach is vacuum neutralization. Here, sources located outside the vacuum beam transport region create the electrons. The electrons join the ions as needed. The resulting neutralized beam has an electron density approximately equal to the beam density [7].

For measuring the ion beam charge neutralization we used a charge collector without magnetic insulation or voltage bias. The diameter of the collector was 8 mm and the diameter of the hole in the lid was 4 mm. The electron current was recorded simultaneously by two collectors, located at a distance of 10 cm downstream from the diode.

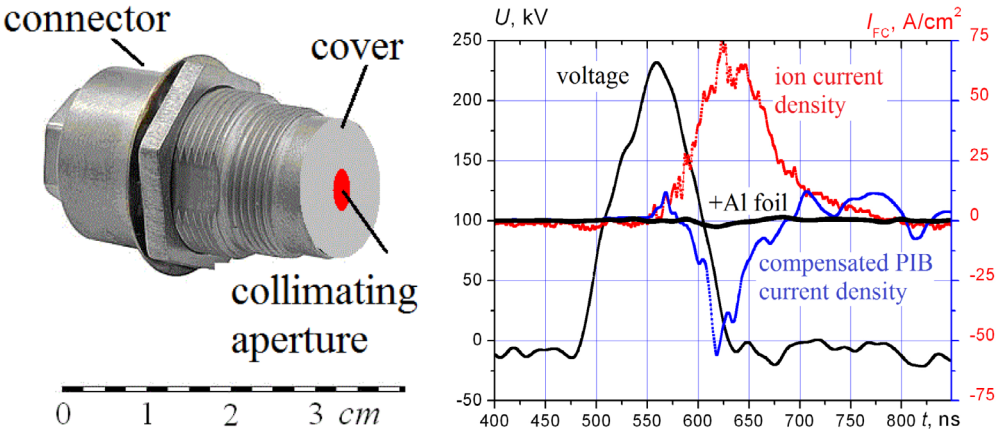

Fig. 13. The construction of a charge collector for measuring ion beam charge neutralization and waveforms of the accelerating voltage (second pulse), ion current density (red line) neutralized beam current density (blue line) and current density, measured by a charge collector, covered with a 10 μ Al foil (black line).

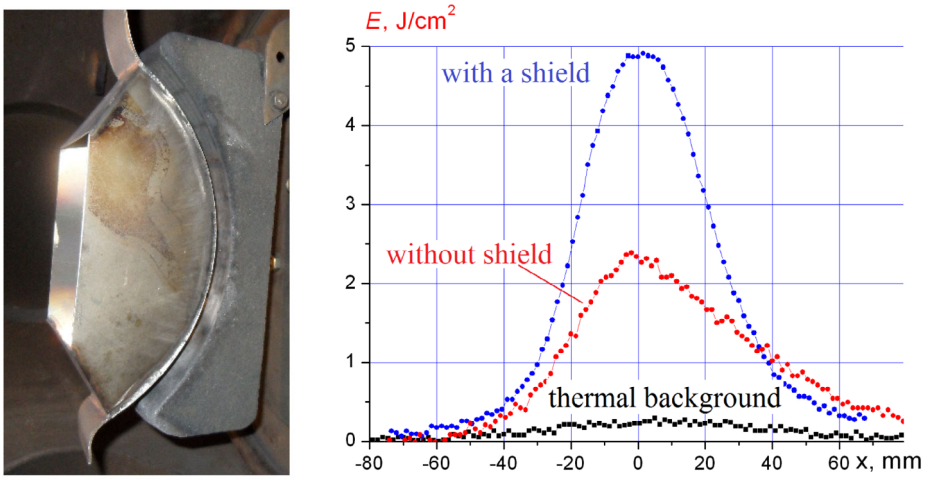

Fig. 14. Photograph of the strip focusing diode with the shield installed on the grounded electrode and the energy-density distribution of the beam, formed by a diode with and without a shield.

The construction of the charge collectors and recorded waveforms of electron current are shown in Figure 13.

Ion current density was measured with a magnetically insulated Faraday cup ($B = 0.4$ T). According to the results of beam space charge compensation measurements the concentration of neutralizing electrons in the focus exceeds the ion concentration by a factor of 1.3–1.5. The electron energy does not exceed 50 keV. We assume that ion beam is supplied with low-energy electrons when passing thought the slits in the grounded electrode. When ions, accelerated by eclectic filed in the diode gap pass though the slits on the grounded electrode the space-charge potential of the ion beam accelerates electrons from the plasma in the slits, which hence provides space charge neutralization of the ion beam.

For increasing ion beam focusing efficiency and preventing the ion loss from the beam volume during propagation to the target, we used a metal shield installed on the grounded electrode. Figure 14 shows the photograph of the strip focusing diode with the shield and energy density distribution on the target installed in the focusing plane.

The shield was made from 1 mm stainless steel foil. The depth of the skin-layer in the metal shield in which magnetic field penetrates is 120 μm. Figure 15 shows a 3-D infrared image of PIB on the target, formed by a strip focusing diode with and without the shield. The distance from the diode to target is 15 cm. Each thermal pattern is obtained for one pulse.

We have showed that the half-height width of the ion beam decreases from 60 mm to 40–42 mm when using the shield. The beam divergence was decreased from 11° to 7.5–8°. It was found that in our experimental conditions magnetic field, formed by the diode self-current penetrates into the plasma of a charge neutralized ion beam to a depth comparable with the half of the beam diameter. The effectiveness of the metal shield we attribute to the elimination of magnetic filed in the beam transport region.

When ion beam prorogates inside the conducting metal shield, installed on the grounded electrode, a mechanism of transverse neutralization might play an important role as well. As explained by Humphries [7] when the beam passes between conducting boundaries that act as electron

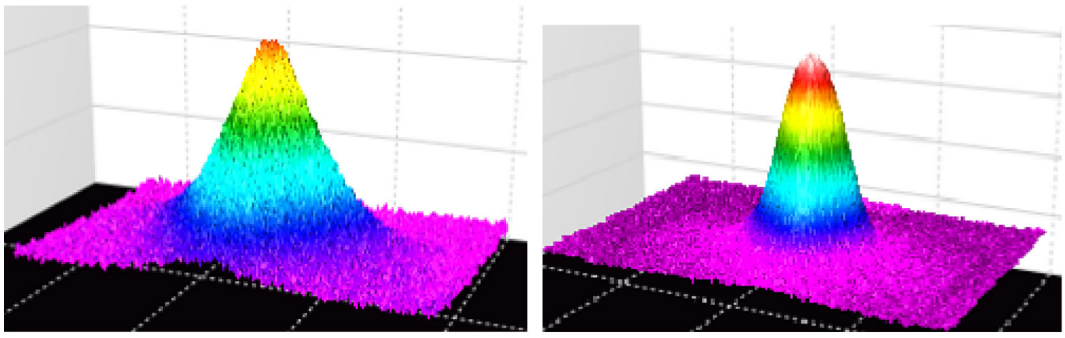

(a) (b)

Fig. 15. Thermal pattern of the ion beam, formed by a focusing diode without a shield (a) and with shield (b).

sources, the space-charge electric field of the ions pulls electrons from the boundaries. Ideally, the electrons cancel electric fields in the beam. In our experimental arrangement these boundaries are the walls of the metal shield.

Thus, in order to achieve effective transportation and focusing of an ion beam in self-magnetically insulated diode it is important to provide conducting boundaries in the beam transport region which serve for both elimination of electromagnetic field in the beam propagation area and supplying ion beam with neutralizing electrons magnetic filed in the beam transport region and realization of the transverse neutralization mechanism.

The combination of high efficiency, when comparable to diodes with external magnetic insulation, good shot-to-shot reproducibility, simplicity of design and configuration, and long service life (more than 10^6 pulses) makes the diode with self-insulation very promising for industrial applications where high-energy beams are used for the surface modification of materials.

7 Conclusion

Complex research was conducted into PIB generation process in self-magnetically insulated diodes. Investigations are performed into diodes of different design: strip focusing and planar diodes, and a new spiral diode. Main results are summarized as follows.

We have designed a new geometry of the diode with a spiral grounded electrode. In a spiral diode it is possible to increase the efficiency from 5–9% (previously studied diodes) up to 20–25%. The high efficiency is achieved due to increase in the length of the electron drift and, consequently, increase in the electron transit time in the spiral diode.

A study on shot to shot variation in energy density of an ion beam formed by a self-magnetically insulated diode revealed that the standard deviation of energy density does not exceed 11%, whilst the same variation for ion current density was 20–30%. The ion current density is only weakly dependant on the accelerating voltage and other output parameters of the accelerator (coefficient of determination <0.3); whilst the correlation between the energy density of the beam and the output parameters is strong (coefficient of determination >0.9).

Focusing properties of an ion beam have been significantly improved by using a metal shield on the grounded electrode. The half-height width of the ion beam decreased from 60 mm to 40–42 mm when using the shield Use of the shield on the grounded electrode provides decrease in the beam divergence from 11° to 7.5–8°. The effectiveness of the metal shield we attribute to both the elimination of

The combination of high efficiency, when comparable to diodes with external magnetic insulation, good shot-to-shot reproducibility, simplicity of design and configuration, and long service life (more than 10^6 pulses) makes the diode with self-insulation very promising for industrial applications where high-energy beams are used for the surface modification of materials.

This research was supported by the grant for scientific research “Science” from the Ministry of Education and Science of Russia, Project No. 3.1301.2014.

References

1. A.D. Pogrebnjak, Utilization of high power ion beams and high current electron beams for modification of metalline materials, *High-Power Particle Beams, 1994 10th International Conference on* (1994), Vol. 1, pp. 232–235
2. S.P. Bugaev, S.D. Korovin, N.N. Koval, E.M. Oks, D.I. Proskurovsky, N.S. Sochugov, *Intense low-energy electron and ion beams and their application Power Modulator Symposium and High-Voltage Workshop. Conference Record* (2002), pp. 548–551
3. D.J. Rej el al., J. Vac. Sci. Technol. A **15**, 1089 (1997)
4. T.J. Renk el al., Proc. IEEE. **92**, 1057 (2004)
5. J. Piekoszewski, Z. Werner, W. Szymczyk, Vacuum. **63**, 475 (2001)
6. V.M. Bystritskii, A.N. Didenko, *High-Power Ion Beams* (American Institute of Physics, New York, 1989)
7. S. Humphries, *Charged Particle Beams* (Wiley, New York, 1990)
8. I. Langmuir, Phys. Rev. **2**, 450 (1913)
9. R.N. Sudan, R.V. Lovelace, Phys. Rev. Lett. **31**, 1174 (1973) R.N. Sudan, R.V. Lovelace, Phys. Rev. Lett. **31**, 1174 (1973)
10. P. Dreike, C. Eichenberger, S. Humphries, R. Sudan, J. Appl. Phys. **47**, 85 (1976)
11. E.G. Furman, A.V. Stepanov, N.Zh. Furman, J. Tech. Phys. **52**, 621 (2007)
12. S. Humphries, Plasma Phys. **19**, 399 (1977)
13. G.A. Mesyats, D.I. Proskurovsky, *Pulsed Electrical Discharge in Vacuum* (Springer-Veriag, New York, 1989)

14. E.I. Logachev, G.E. Remnev, U.P. Usov, Tech. Phy. Lett. **6**, 1404 (1980)
15. G.E. Remnev et al., Surf. Coat. Technol. **114**, 206 (1999)
16. Ya.E. Krasik, A. Dunaevsky, A. Krokhmal, J. Felsteiner, A.V. Gunin, I.V. Pegel, S.D. Korovin, J. Appl. Phys. **89**, 2379 (2001) and references therein
17. A.I. Pushkarev, J.I. Isakova, M.S. Saltimakov, R.V. Sazonov, Nat. Sci. **2**, 419 (2010)
18. A.I. Pushkarev, Yu.I. Isakova, I.P. Khailov, Tech. Phys. Lett. **40**, 565 (2014)
19. A. Pushkarev, Yu. Isakova, Surf. Coat. Technol. (2012)
20. Y.I. Isakova, A.I. Pushkarev, I.P. Khaylov, Rev. Sci. Instrum. **84**, 073302 (2013)
21. Y.I. Isakova, A.I. Pushkarev, I.P. Khaylov, Rev. Sci. Instrum. **85**, 073303 (2014)
22. Yu.I. Isakova, J. Korean Phys. Soc. **59**, 3531 (2011)
23. A.I. Pushkarev, J.I. Isakova, M.S. Saltimakov, R.V. Sazonov, Phys. Plasmas **17**, 013104 (2010)
24. Yu.I. Isakova, A.I. Pushkarev, Instrum. Exp. Tech. **56**, 185 (2013)
25. Yu. Isakova, G. Kholodnaya, I. Alexander, Adv. High Energy Phys. (2011), Article ID 649828
26. QuickField 5.10: Finite Element Analysis package for electromagnetic, thermal, and stress design simulation
27. J.P. Vandevender, J.P. Quintenz, R.J. Leeper, D.J. Johnson, J.T. Crow, J. Appl. Phys. 4 (1981)
28. K.W. Zieher, Nucl. Instrum. Methods Phys. Res. **228**, 161 (1984)
29. V.M. Bystritskii, Yu.A. Glushko, A.V. Kharlov, A.A. Sinebryukhov, Laser Particle Beams **9**, 691 (1991)
30. V.M. Bystritskii, A.N. Didenko, Y.E. Krasik, V.M. Matvienko, Plasma Phys. **11**, 1057 (1985)
31. T. Yoshikawa, K. Masugata, M. Ito, M. Matsui, K. Yatsui, J. Appl. Phys. **56**, 3137 (1984)
32. A.I. Pushkarev, Yu.I. Isakova, Tech. Phys. **57**, 181 (2012)
33. A.I. Pushkarev, Yu.I. Isakova, Laser Particle Beams **30**, 427 (2012)
34. A.I. Pushkarev, Y.I. Isakova, Closed electron drift in a self-magnetically insulated ion diode, Phys. Plasmas
35. X.P. Zhu, M.K. Lei, Z.H. Dong, T.C. Ma, Rev. Sci. Instrum. **74**, 47 (2003)
36. X.P. Zhu, Z.H. Dong, X.G. Han, J.P. Xin, M.K. Lei, Rev. Sci. Instrum. **78**, 023301 (2007)
37. H. Ito, H. Miyake, K. Masugata, Rev. Sci. Instrum. **79**, 103502 (2008)
38. A.I. Pushkarev, Yu.I. Isakova, I.P. Khailov, Rev. Sci. Instrum. **83**, Article ID 073309 (2012), DOI: 10.1063/1.4737186, http://link.aip.org/link/?RSI/83/073309
39. H.A. Davis, R.R. Bartsch, J.C. Olson, D.J. Rej, W.J. Waganaar, J. Appl. Phys. **82**, 3223 (1997)
40. A.I. Pushkarev, Yu.I. Isakova, I.P. Khailov, Y. Xiao, Rev. Sci. Instrum. **84**, 083304 (2013)
41. C.L. Olson, J. Fusion Energy **1**, 309 (1982)
42. K. Yatsui, A. Tokuchi, H. Tanaka, H. Ishizuka, A. Kawai, E. Sai, K. Masugata, M. Ito, M. Matsui, Laser Particle Beams **3**, 119 (1985)
43. W. Bauer, A. Citron, W. Kihhn, A. Rogner, W. Schimassek, O. Stoltz, Investigation of a self-magnetically insulated Bθ-diode, in *Proceeding of the 6th IEEE International Pulsed Power Conference* (Arlington, Virginia, 1987), pp. 244–247
44. K.W. Zieher, Nucl. Instrum. Methods **228**, 169 (1984)